# Search for $D^0$-$\overline{D^0}$ Mixing with Double-Layer TOF at BESⅢ *

SUN Yong-Zhao[1,2;1)] HE Kang-Lin[1;2)] LI Wei-Dong[1;3)] BIAN Jian-Ming[1,2] CAO Guo-Fu[1,2]
DENG Zi-Yan[1] HE Miao[1,2] HUANG Bin[1,2] JI Xiao-Bin[1] LI Gang[1,3] LI Hai-Bo[1] LIU Chun-Xiu[1]
LIU Huai-Min[1] MA Qiu-Mei[1] MA Xiang[1,2] MAO Ya-Jun[4] MAO Ze-Pu[1] MO Xiao-Hu[1] QIU Jin-Fa[1]
SUN Sheng-Sen[1] WANG Ji-Ke[1,2] WANG Liang-Liang[1,2] WEN Shuo-Pin[1] WU Ling-Hui[1,2]
XIE Yu-Guang[1,2] YANG Ming[1,2] YOU Zheng-Yun[4] YU Guo-Wei[1] YUAN Chang-Zheng[1]
YUAN Ye[1] ZANG Shi-Lei[1,3] ZHANG Chang-Chun[1] ZHANG Jian-Yong[1,3] ZHANG Ling[5]
ZHANG Xue-Yao[6] ZHANG Yao[6] ZHENG Zhi-Peng[1] ZHU Yong-Sheng[1] ZOU Jia-Heng[6]

1 (Institute of High Energy Physics, CAS, Beijing 100049, China)
2 (Graduate University of Chinese Academy of Sciences, Beijing 100049, China)
3 (CCAST(World Laboratory), Beijing 100080, China)
4 (Peking University, Beijing 100871, China)
5 (Hunan University, Changsha 410082, China)
6 (Shandong University, Ji'nan 250100, China)

**Abstract** The decay of $D^0 \to K^-\pi^+$ is a golden channel in the study of $D^0$-$\overline{D^0}$ mixing at ψ(3770). The requirements of excellent K/π separation will play an essential role in the mixing search. A technique was developed to precisely extract event start time ($t_0$) with TOF measurements in multiple charged tracks event at BESⅢ. After the $t_0$ extracting algorithm, the time resolution of double-layer TOF reduced from ~78ps to ~64ps, the upper limit of $D^0$-$\overline{D^0}$ mixing rate at 95% CL can be improved by a factor of 7% in 20fb$^{-1}$ ψ(3770) data.

**Key words** $D^0$-$\overline{D^0}$ mixing, $D^0 \to K^-\pi^+$, particle identification, TOF, event start time

## 1 Introduction

In the Standard Model(SM), $D^0$-$\overline{D^0}$ mixing is generated by short distance diagrams including the one shown in Fig. 1. The heaviest off-shell intermediate quark is the b. The mixing rate goes as the square of the mass of the intermediate quark, we can see $D^0$ mixing is highly suppressed relative to $K^0$ mixing or $B^0$ mixing, since the top quark is active in these systems. Mixing due to natural causes in the Standard Model can be enhanced by the so-called "long distance effects", which are more-or-less the transition of a $D^0$ into an on-shell meson pair, such as $K^+K^-$

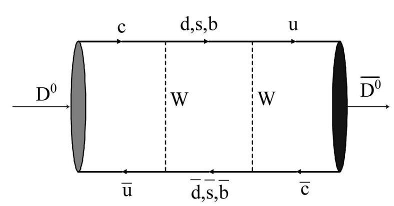


Fig. 1. A diagram for $D^0$-$\overline{D^0}$ mixing in the Standard Model.

with the mass $m_{K^+K^-} = m_{D^0}$ and then transition back to a $\overline{D^0}$. Mixing is characterized by the mass def-

Received 29 August 2006, Revised 30 October 2006
* Supported by CAS Knowledge Innovation Project(U-602, U-34), National Natural Science Foundation of China (10491300, 10605030) and 100 Talents Program of CAS (U-25, U-54)

1) E-mail: sunyz@ihep.ac.cn
2) E-mail: hekl@ihep.ac.cn
3) E-mail: liwd@ihep.ac.cn

erence, $\Delta m$, and the width difference $\Delta\Gamma$, between $CP+$ and $CP-$ eigenstates.

$$x=\frac{\Delta m}{\Gamma}\ ,\qquad y=\frac{\Delta\Gamma}{\Gamma}\ , \tag{1}$$

where the width $\Gamma$ is related to the lifetime, $\tau_{\mathrm{D}^0}$, as $\Gamma\cdot\tau_{\mathrm{D}^0}=\hbar$. The mixing rate $R_{\mathrm{M}}$ is approximately

$$R_{\mathrm{M}}=\frac{x^2+y^2}{2}\ . \tag{2}$$

The prediction of $x$ and $y$ in the Standard Model, varies by several orders of magnitudes ($10^{-7}$—$10^{-2}$)[1—7]. Several non-standard models predict $|x|>0.01$. Contributions to $x$ at this level could result from the new physics effects in loops, for example new particles with masses as high as 10—100 TeV[8, 9].

The parameters $x$ and $y$ can be measured in variety of ways. The most popular measurements in recent years, are obtained by exploiting the time-dependence of D decays, including: the measurement of the wrong-sign semileptonic branching ratio $\mathrm{D}^0\to\mathrm{K}^+\mathrm{l}^-\overline{\nu_{\mathrm{l}}}$, which is sensitive to $R_{\mathrm{M}}$; decay rates to CP eigenstates $\mathrm{D}^0\to\mathrm{K}^+\mathrm{K}^-$ and $\pi^+\pi^-$, which are sensitive to $y$; the wrong sign $\mathrm{D}^0\to\mathrm{K}^+\pi^-$ hadronic branching ratio, which is sensitive to $x'^2=(y\sin\delta_{\mathrm{K}\pi}+x\cos\delta_{\mathrm{K}\pi})^2$ and $y'=y\cos\delta_{\mathrm{K}\pi}-x\sin\delta_{\mathrm{K}\pi}$, where $\delta_{\mathrm{K}\pi}$ is the relative strong phase between $\mathrm{D}^0$ and $\overline{\mathrm{D}^0}$ decay to $\mathrm{K}^+\pi^-$; and the decay rate of $\mathrm{D}^0\to\mathrm{K}^0_{\mathrm{s}}\pi^+\pi^-$, which determines the strong phase $\delta_{\mathrm{K}^0_{\mathrm{s}}\pi^+\pi^-}$ from a Dalitz analysis and measures $x$ and $y$. The most precise constraints[10] on $x'$ and $y'$ are drawn in Fig. 2, $|x|\sim|y|$ are of order $10^{-3}$—$10^{-2}$. By the limits of current experimental sensitivity, $\mathrm{D}^0$ mixing has not been observed.

The upgraded Beijing Electron Positron collider(BEPCⅡ) will run in $E_{\mathrm{cm}}$=2—4.2GeV energy region, with a designed luminosity of $1\times10^{33}\mathrm{cm}^{-2}\cdot\mathrm{s}^{-1}$ at a beam energy of 1.89GeV, for the precision τ-charm physics studies. Running at Charm threshold can provide extremely clean and pure charm events. Time-dependent analyse are not feasible at BESIII; However, the quantum cohenrence of the two initial state D mesons for ψ(3770) allows both simple and sophisticated methods to measure $\mathrm{D}^0$-$\overline{\mathrm{D}^0}$ mixing paramters, strong phase, CP eigenstate branching fractions and CP violation[11, 12]. For instance, any observation of $(\mathrm{K}^\mp\pi^\pm)(\mathrm{K}^\mp\pi^\pm)$ double tag event at ψ(3770) means an unambiguous evidence of $\mathrm{D}^0$-$\overline{\mathrm{D}^0}$ mixing. In this paper, we present a Monte Carlo study for searching $(\mathrm{K}^\mp\pi^\pm)(\mathrm{K}^\mp\pi^\pm)$ events using double-layer TOF at BESⅢ.

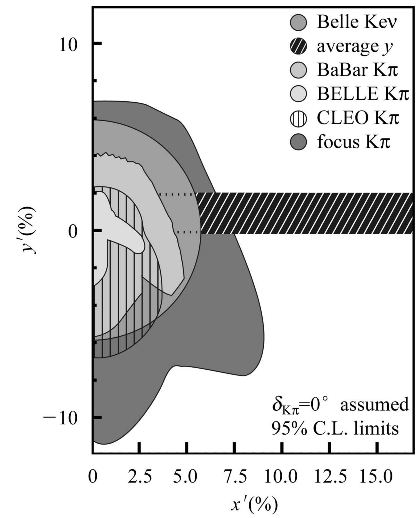


Fig. 2. Allowed region in $x'y'$ plane. The allowed region for $y$ is the average of the results from several experiments.

## 2 The BESⅢ detector

The BESⅢ detector[13, 14] consists of a berylium beam pipe, a helium-based small cell drift chamber, Time-of-Flight (TOF) counters for particle identification, a CsI(Tl) crystal calorimeter, a superconducting solenoidal magnet with a field of 1T, and a muon identifier using the magnet yoke interleaved with Resistive Plate Counters (RPC).

There are 43 layers of sensitive wires in the main drift chamber (MDC). The polar angle coverage is $|\cos\theta|=0.83$ for a track passing through all layers, and $|\cos\theta|=0.93$ for one that passes through 20 layers. The expected spatial, momentum, and $\mathrm{d}E/\mathrm{d}x$ resolution are $\sigma_{\mathrm{s}}=130\mu\mathrm{m}$, $\sigma_{\mathrm{p}}/p$=0.5% at 1GeV/$c$, and $\sigma_{\mathrm{d}E/\mathrm{d}x}/\mathrm{d}E/\mathrm{d}x\sim6\%$, respectively. Outside the MDC is the time-of-flight system, which is crucial for particle identification. It consists of a two-layer barrel array and one-layer endcap arrays of scintillators. The expected time resolution for kaon and pion is 100—110ps, giving a 2σ K/π separation up to 0.9GeV/$c$ for normal tracks. The CsI(Tl) crystal calorimeter constains 6240 crystals with a length of 28cm or 15 radiation lengths. The expected energy and spatial resolutions at 1GeV are 2.5% and 0.6cm, respectively. The super-conducting magnet is a 3.91m long single layer solenoid with a magnetic field of 1T. The magnet return iron has 9 layers of Resistive Plate Chambers (RPC) in the barrel and 8 layers in the endcap to form a muon detector. The spatial resolution of muon counter is about 16.6mm.

The trigger system is pipelined and uses FPGAs. The information from the TOF, MDC, and muon counter will be used. The maximum trigger rate at the J/ψ will be about 4000Hz with a good event rate of about 2000Hz. The whole data acquisition system has been tested to 8kHz for an event size of 12kb. The expected bandwidth after level one is 48Mbytes/s. The preliminary version of the BES Offline Software System(BOSS)[15] is complete. A tremendous amount of work has been accomplished but much remains to be done. The detector simulation[16] is based on Geant4[17].

## 3 Determination of the $t_0$ in multiple charged tracks event

The momentum of final particles in the decay of $D^0 \to K^-\pi^+$ at ψ(3770) is shown in Fig. 3, ranging from 0.7 to 1.05GeV. d$E$/d$x$ cannot separate K/π very well in these momentum regions, the requirement of excellent K/π separation using TOF counter will play an essential role in searching for $D^0$-$\overline{D^0}$ mixing with the decay of $D^0 \to K^-\pi^+$ at BESIII.

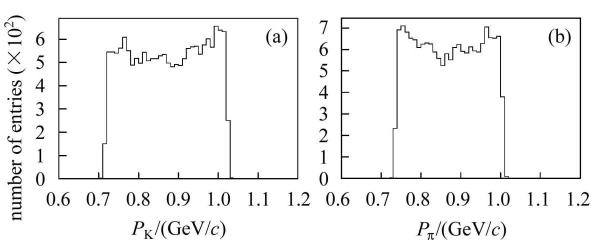


Fig. 3. (a) $p_K$ and (b) $p_\pi$ distributions in the decay of $D^0 \to K^-\pi^+$.

### 3.1 Particle identification using TOF counter

The physics target of the TOF system is to measure the flight time of charged particles for particle identification (PID) by comparing the measured time

$$t_{\rm mea} = {\rm TDC} - t_0 - t_{\rm cor}$$

against the predicted time

$$t_{\rm exp} = \frac{L}{\beta c}, \quad \beta = \frac{p}{\sqrt{p^2+m^2}} ,$$

where TDC is the time value recorded by TOF electronics, $t_0$ is the collision time, the so-called “event start time”, $t_{\rm cor}$ is the correction term from calibration, $c$ is the velocity of light, $m$ is the mass of charged particle, $\beta$ is the flight velocity of charged particle. $L$ and $p$ are the flight path and the momentum of charged particle gived by the MDC measurements.

The accurate determination of the $t_{\rm mea}$ requires that both the beginning and end-time of charged track flight be determined accurately. The end-time is measured by the TOF counter. $t_{\rm cor}$ is carefully calibrated with the known data type, such as Bhabha events, in offline reconstruction and physics analysis. The detailed information about TOF calibration and correction procedure are described elsewhere[18—20]. The precision of beginning time is controlled by the accuracy of $t_0$. BEPCII will operate with a bunch crossing time of 8ns, the Trigger-DAQ system can identify the bunch cross number within 3 collision periods. The exact bunch cross number, is obtained[21] during the offline tracking and TOF reconstruction.

The PID ability depends on the time resolution of the TOF system. There are many sources which affect the BESIII TOF measurement[13]: the intrinsic time resolution of TOF is related to the scintillator and the PMT performance; the contribution from TOF electronics, including the precision of TDC and the time-walk effects; additional uncertainties caused by flight path calculation and the precision of hit position predicted by MDC track extrapolation; the collision time of electron and positron depends on the bunch time and bunch length.

The time resolution is expected to be about 100ps for a single TOF counter. The time resolution for the double-layer TOF in barrel cannot be simply reduced by a factor of $1/\sqrt{2}$ from the one for single layer, due to the correlation of common factors which contribute to each of the measured time-of-flight, such as the event start time($t_0$). The average resolution of $t_0(\sigma_{t_0})$ could be determined by analyzing the two-end readout data of barrel TOF counter[22], and will be applied to the $t_{\rm mea}$ reconstruction[23].

### 3.2 The $t_0$ extracting algorithm

In one $e^+e^-$ collision, all produced particles fly from the interaction point (IP) toward the outer detector. For TOF measurement, the fact that all $t_{\rm mea}$'s of charged tracks have a common $t_0$ in one event can be used to set up the following constraints equation

$$H(\alpha,t_0)=\begin{pmatrix}\alpha_1-t_0\\ \alpha_2-t_0\\ \cdots\cdots\\ \alpha_n-t_0\end{pmatrix}=0\ , \tag{3}$$

where $\alpha$ is a vector of $\alpha_i$'s, the expected $i$-th $\Delta t = t_{\rm mea}-t_{\rm exp}$ of TOF measurement for charged track; the event start time $t_0$ is an unknown parameter. The solution of Eq. (3) is a typical problem of the least square fit with constraints and unknown parameters. The fitting technique is straight and is based on the well-known Lagrange multiplier method[24].

In general case, let $\alpha$ represent the $n$ TOF measurements, $t$ represent the $m$ unknown parameters, and $H(\alpha,t)$ represent the $r$ constraints equation. Thus $\alpha$, $t$ and $H$ have the form of column vectors

$$\alpha=\begin{pmatrix}\alpha_1\\ \alpha_2\\ \vdots\\ \alpha_n\end{pmatrix},\quad H=\begin{pmatrix}H_1\\ H_2\\ \vdots\\ H_r\end{pmatrix},\quad t=\begin{pmatrix}t_1\\ t_2\\ \vdots\\ t_m\end{pmatrix}\ . \tag{4}$$

The constraints equation can be linearized and summarized in three matrices:

$$D=\begin{pmatrix}\frac{\partial H_1}{\partial\alpha_1} & \frac{\partial H_1}{\partial\alpha_2} & \cdots & \frac{\partial H_1}{\partial\alpha_n}\\ \frac{\partial H_2}{\partial\alpha_1} & \frac{\partial H_2}{\partial\alpha_2} & \cdots & \frac{\partial H_2}{\partial\alpha_n}\\ \vdots & \vdots & \ddots & \vdots\\ \frac{\partial H_r}{\partial\alpha_1} & \frac{\partial H_r}{\partial\alpha_2} & \cdots & \frac{\partial H_r}{\partial\alpha_n}\end{pmatrix}\ , \tag{5}$$

$$E=\begin{pmatrix}\frac{\partial H_1}{\partial t_1} & \frac{\partial H_1}{\partial t_2} & \cdots & \frac{\partial H_1}{\partial t_m}\\ \frac{\partial H_2}{\partial t_1} & \frac{\partial H_2}{\partial t_2} & \cdots & \frac{\partial H_2}{\partial t_m}\\ \vdots & \vdots & \ddots & \vdots\\ \frac{\partial H_r}{\partial t_1} & \frac{\partial H_r}{\partial t_2} & \cdots & \frac{\partial H_r}{\partial t_m}\end{pmatrix}\ , \tag{6}$$

and

$$d=\begin{pmatrix}H_1\\ H_2\\ \vdots\\ H_r\end{pmatrix}\ . \tag{7}$$

The $\chi^2$ can be constructed as a sum of two terms

$$\begin{aligned}\chi^2 =\ & (\alpha-\alpha_0)^{\rm T}V_{\alpha_0}^{-1}(\alpha-\alpha_0)+\\ & 2\lambda^{\rm T}(D\delta\alpha+E\delta t+d)\end{aligned} \tag{8}$$

where $\alpha_0$ and $V_{\alpha_0}$ are the initial values of $\alpha$ and its covariance matrix. $\delta\alpha=\alpha$–$\alpha_A$ and $\delta t = t$–$t_{\rm A}$, the departures of the variables from their expansion point $A$, the Lagrange multipliers $\lambda$ is a vector of $r$ unknowns. Let $\partial\chi^2/\partial\alpha=0$, $\partial\chi^2/\partial t=0$ and $\partial\chi^2/\partial\lambda=0$, we get

$$\begin{gathered}V_{\alpha_0}^{-1}(\alpha-\alpha_0)+D^{\rm T}\lambda=0\ ,\\ E^{\rm T}\lambda=0\ ,\\ D\delta\alpha_0+E\delta t_0+d=0\ .\end{gathered} \tag{9}$$

where $\delta\alpha_0=\alpha_0$–$\alpha_{\rm A}$, $\delta t_0=t_0$–$t_{\rm A}$, $t_0$ is the initial value of $t$. The solution of Eq. (9) is straight forward[25]

$$\begin{aligned}\delta t_0 &= -V_{t_0}E^{\rm T}\lambda_0\ ,\\ V_{t_0} &= (E^{\rm T}V_{\rm D}E)^{-1}\ ,\\ \lambda_0 &= V_{\rm D}(D\delta\alpha_0+d)\ ,\\ V_{\rm D} &= (DV_{\alpha_0}D^{\rm T})^{-1}\ ,\end{aligned} \tag{10}$$

where $\lambda_0$ is an $r$-dimension column vector, $V_{\rm D}$ is an $r\times r$ matrix, $V_{t_0}$ is an $m\times m$ matrix. The updated $\alpha$ and $\chi^2$ are given by:

$$\begin{aligned}\alpha &= \alpha_0-V_{\alpha_0}D^{\rm T}\lambda\ ,\\ \lambda &= \lambda_0+V_{\rm D}E\delta t_0\ ,\\ \chi^2 &= \lambda^{\rm T}(D\delta\alpha_0+d)\ .\end{aligned} \tag{11}$$

### 3.3 Extracting $t_0$ with Toy Monte Carlo data

For BESIII TOF measurements, applying $m=1$ and $r=n$ to Eqs. (3)—(7), the related matrices have the following forms:

$$D=\begin{pmatrix}1 & & & \\ & 1 & & \\ & & \ddots & \\ & & & 1\end{pmatrix},\qquad E=\begin{pmatrix}-1\\-1\\\vdots\\-1\end{pmatrix},$$

$$d=\begin{pmatrix}\alpha_1-t_0\\\alpha_2-t_0\\\vdots\\\alpha_n-t_0\end{pmatrix},\quad V_{\alpha_0}=\begin{pmatrix}\sigma_{t1}^2 & \sigma_{t_0}^2 & \dots & \sigma_{t_0}^2\\ \sigma_{t_0}^2 & \sigma_{t_2}^2 & \dots & \sigma_{t_0}^2\\ \vdots & \vdots & \ddots & \vdots\\ \sigma_{t_0}^2 & \sigma_{t_0}^2 & \dots & \sigma_{tn}^2\end{pmatrix},\tag{12}$$

where $D$ a $n\times n$ unitary matrix, $E$ a $1\times n$ matrix, $d$ a $n$-dimension column vector, $V_{\alpha_0}$ a $n\times n$ matrix. $\sigma_{t_i}$ and $\sigma_{t_0}$ represent the total time resolution of $i$th $t_{\rm mea}$ and the resolution of average $t_0$. The non-diagonal elements ($\sigma_{t_0}$) which appeared in matrix $V_{\alpha_0}$ represent the correlation between TOF measurements due to the uncertainty of $t_0$.

The $t_0$ extracting algorithm is written in C++ Language using CLHEP[26] package. The calculations are based on Eqs. (3)—(12). To check the algorithm, Toy Monte Carlo data with four charged tracks (8 TOF measurements) were generated according to the parameters from the Geant4[17] based full BESIII detector simulation[16], e.g., time resolution of $\sim$ 90ps for inner layer TOF, $\sim$ 100ps for outer layer TOF, and $\sim$35ps for $t_0$ uncertainty. Fig. 4 shows the comparison of generated and extracted $t_0$ with Toy Monte Carlo data. The difference is small enough (within several ps) and could be ignored. After $t_0$ extracting, the time resolution was significantly improved which we'll show in the next section with the full simulated $D^0$-$\overline{D^0}$ mixing events.

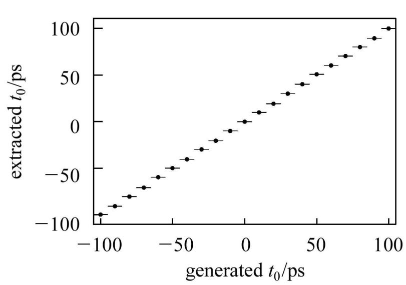


Fig. 4. Comparison of generated $t_0$ and extracted $t_0$ with 10 000 Toy Monte Carlo data. The offset of $t_0$ are scanned from −100ps to 100ps.

## 4 Search for $D^0$-$\overline{D^0}$ mixing using the decay of $D^0\to K^-\pi^+$

At $\psi(3770)(J^{PC}=1^{--})$, $D^0\overline{D^0}$ pair will be produced in $C=-1$ state. There are two paths for $D^0\to K^+\pi^-$ in which $D^0$ decays like $\overline{D^0}$: (1) through Double Cabbibo Suppressed Decay (DCSD); (2) through $D^0$-$\overline{D^0}$ mixing. For the process of $e^+e^-\to\psi(3770)\to D^0\overline{D^0}\to(K^-\pi^+)_1(K^-\pi^+)_2$, $(K^-\pi^+)_1$ and $(K^-\pi^+)_2$ systems have the identical final states and can be regarded as identical particles, their coherent wave function must be symmetric and have a charged parity $C=+1$ by the requirement of Bose-Einstein statistics. Therefor for $C=-1$ coherent state $\psi(3770)\to D^0\overline{D^0}$, DCSD cannot contribute to $\overline{D^0}\to K^-\pi^+$. Hence, tagging $(K^-\pi^+)(K^-\pi^+)$ or $(K^+\pi^-)(K^+\pi^-)$ events at $\psi(3770)$ would be an unambiguous evidence for existence of $D^0$-$\overline{D^0}$ mixing. The mixing parameter $R_{\rm M}$ can be measured through

$$R_{\rm M}\approx\frac{\Gamma(D^0\to K^+\pi^-)}{\Gamma(D^0\to K^-\pi^+)}\ .\tag{13}$$

### 4.1 Event selection

Four charged tracks in $(K\pi)(K\pi)$ final states are required to be from IP and to pass a common vertex constraint. A charged track is identified as either kaon or pion, if the measured energy loss in drift chamber agrees with that predicted for a kaon or pion within three standard deviations, identification to either kaon or pion is allowed. At least one TOF hit is required for each track, but the TOF information is not used for particle identification at this step. Appropriate combinations of $K\pi$ pair are constructed as a $D^0\to K^-\pi^+$ tag.

Good background rejection can be achieved with the requirement of $\Delta E=E_{\rm rec}-E_{\rm beam}$, the difference between reconstructed energy of D tags ($E_{\rm rec}$) and the beam energy ($E_{\rm beam}$). As shown in Fig. 5, a requirement on $\Delta E$ can help to remove single misidentification backgrounds very easily. The dominant background comes from a double interchanges of $(K^-\pi^+)(\pi^+K^-)$ events, which cannot be completely rejected by a stringent $\Delta E$ cut(<0.02GeV).

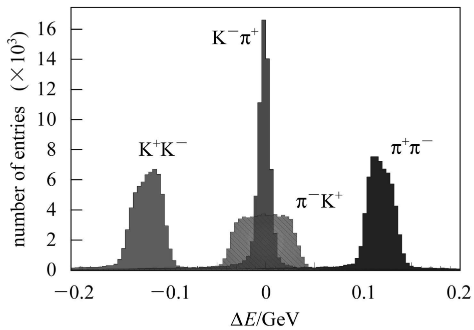


Fig. 5. $\Delta E$ distribution for decay of $D^0 \rightarrow K^-\pi^+$, single misidentification decay of $D^0 \rightarrow K^+K^-$ and $D^0 \rightarrow \pi^+\pi^-$, and double misidentification decay of $\overline{D^0} \rightarrow K^+\pi^-$.

All (Kπ) pairs are subjected to the kinematic fit for the hypothesis:

$$\psi(3770) \rightarrow D^0\overline{D^0} \rightarrow (K\pi)_1(K\pi)_2$$

with the equal mass constraint $M_1 = M_2$ (the mass is not fixed at $M_{D^0}$). Energy-momentum conservation for $D\overline{D}$ production provides five constraints. Combinations are required to have the probability of kinematic fit greater than 1%.

The backgrounds' contamination, e.g. coming from $K^-\pi^+\pi^0$ and $K^-l^+\nu_l$ events with a lost $\pi^0$ or an escaped neutrino, can be easily removed by $\Delta E$ cut and kinematic fit. Monte Carlo studies show that the background rates from this kind of events are lower than $10^{-6}$, and could be ignored. To remove the double-misidentification backgrounds, the remained (Kπ)(Kπ) combinations are subjected to the $t_0$ extracting process. The combination with the lowest $\chi^2$ is regarded as the "real" (Kπ)(Kπ) event.

### 4.2 Results

The resulting $t_0$ distribution is drawn in Fig. 6(a). Since the correlation with $t_{\rm mea}$'s, the extracting algorithm will introduce additional uncertainties to $t_0$. ~47ps were estimated according to Eq. (10), a little bit smaller than the values obtained from Fig. 6(a), which was raised by the non-zero offset in $t_{\rm mea}$'s. The combined $\Delta t = (\Delta t_1 + \Delta t_2)/2$ for the two-layer barrel TOF counter are shown in Fig. 6(b) and Fig. 6(c). After the $t_0$ extracting algorithm, the time resolution of two-layer TOF has been improved significantly, from ~78ps to ~64ps. As shown in Fig. 7[27], the background contamination rate is reduced to about half while applying the $t_0$ extracting algorithm in $D^0$-$\overline{D^0}$ mixing using $D^0 \rightarrow K^-\pi^+$ mode at BESIII.

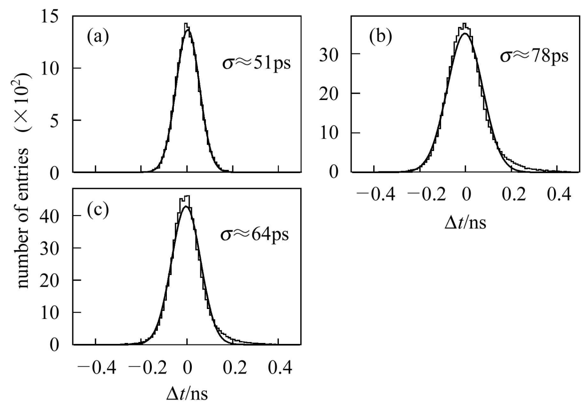


Fig. 6. (a) Distribution of extracted $t_0$ in $D^0\overline{D^0} \rightarrow (K^-\pi^+)(K^+\pi^-)$ events; (b) and (c) combined $\Delta t$ of two-layer TOF measurements without/with $t_0$ extracting algorithm, respectively. The histograms are fitted with a Gaussian function.

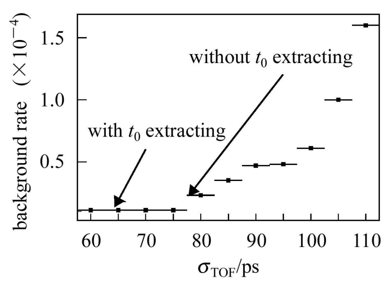


Fig. 7. Double misidentification rate vs the time resolution of combined two-layer TOF while searching the $D^0$-$\overline{D^0}$ mixing using $D^0 \rightarrow K^-\pi^+$ mode at BESIII.

About $2\times10^7$ $D^0\overline{D^0}$ pairs will be produced in one year's data (~5fb$^{-1}$) taking at BESIII, corresponding to $\sim 6.4\times10^3$ $(K^-\pi^+)(K^+\pi^-)$ events (the acceptance is about 20%), which are expected to be obtained. The number of observed $K^\mp\pi^\pm$ vs $K^\mp\pi^\pm$ events can be expressed as:

$$n = N_{(K^-\pi^+)(K^-\pi^+)} = (R_M + \eta)\cdot N_{(K^-\pi^+)(K^+\pi^-)}, \quad (14)$$

where $R_M$ the mixing rate, $\eta$ the background rate due to double misidentification. Table 1 lists the expected mixing signal $s$, background contamination $b$, and the Poisson probability $P(n)$ of observed events number in 20fb$^{-1}$ $\psi(3770)$ data at BESIII under the assumption of $R_M = 10^{-4}$ and $R_M = 10^{-6}$. The statistics of the number of observed events ($n$) in Table 1 is not enough to give a clear measurements of mixing rate if $R_{\mathrm{M}}$ is as low as $10^{-4}$. The Feldman method[28] was used to transfer $n$ to $n_{0.95}$, the upper limit at 95% confidence level (CL). The average $N_{0.95}$ is determined by

$$N_{0.95} = \sum_n n_{0.95} \cdot P(n) \ . \tag{15}$$

According to Eq. (14), Eq. (15) and the $P(n)$ listed in Table 1, the calculated upper limits of $R_{\mathrm{M}}$ at 95% CL with and without $t_0$ correction are listed in the last row of Table 1.

Table 1. The expected mixing signal $s$, background contamination $b$, and the Poisson probabilities $P(n)$ of observed events number in 20fb$^{-1}$ ψ(3770) data at BESIII, where the rate of $D^0$-$\overline{D^0}$ mixing $R_{\mathrm{M}}$ are assumed to be $10^{-4}$ and $10^{-6}$. The upper limit of $R_{\mathrm{M}}$ at 95% CL are listed in the last row. In 2nd row, $Y/N$ mean that the $t_0$ extracting algorithm is/not applied in the analysis.

| $R_{\mathrm{M}}$ | $10^{-4}$ | | $10^{-6}$ | |
|---|---|---|---|---|
| $t_0$ corr | $Y$ | $N$ | $Y$ | $N$ |
| $s$ | 2.56 | 2.56 | 0.03 | 0.03 |
| $b$ | 0.32 | 0.64 | 0.32 | 0.64 |
| $P(0)$ | 5.6% | 4.1% | 70.5% | 51.2% |
| $P(1)$ | 16.2% | 13.0% | 24.7% | 34.3% |
| $P(2)$ | 23.3% | 20.9% | 4.3% | 11.5% |
| $P(3)$ | 22.3% | 22.3% | 0.5% | 2.6% |
| $P(4)$ | 16.1% | 17.8% | | 0.4% |
| $P(5)$ | 9.3% | 11.4% | | |
| $P(6)$ | 4.4% | 6.1% | | |
| $P(7)$ | 1.8% | 2.8% | | |
| $P(8)$ | 0.7% | 1.1% | | |
| $P(9)$ | 0.2% | 0.4% | | |
| $R_{\mathrm{M}}(\times 10^{-4})$ at 95% CL | 3.0 | 3.1 | 1.4 | 1.5 |

As shown in Table 1, the upper limit of $R_{\mathrm{M}}$ at 95% CL is improved (3−7)% in 20fb$^{-1}$ ψ(3770) data at BESIII if $R_{\mathrm{M}}$ is in the order of $10^{-4}$—$10^{-6}$ while applying the $t_0$ extracting algorithm in $D^0 \to K^-\pi^+$ channel. The algorithm can be applied to other interesting modes: $(K^{\mp}l^{\pm}\nu_l)(K^{\mp}l^{\pm}\nu_l)$, which determine the $R_{\mathrm{M}}$ as the same order as $K^-\pi^+$ mode; $(K^{\mp}\pi^{\pm})(K^+K^-)$ and $(K^{\mp}\pi^{\pm})(\pi^+\pi^-)$, which measure the $\delta_{K\pi}$ and determine $y$ in the order of $10^{-4}$; Dalitz analysis of $D^0 \to K^-\pi^+\pi^0$ and $D^0 \to K^0_s\pi^+\pi^-$, which can determine $R_{\mathrm{M}}$ in $K^{\mp}\rho^{\pm}$ and $K^{*\mp}\pi^{\pm}$ modes; the Quantum Coherent Analysis (TQCA), which can improve the mixing parameters more precisely[11]. Combining the above analysis, the sensitivity to $R_{\mathrm{M}}$ could reach to $10^{-5}$ level, very hopefully to "confirm" the $D^0$-$\overline{D^0}$ mixing at BESIII.

## 5 Summary

The BESIII detector with higher luminosity will contribute greatly to the precision measurements in charmonium and flavor physics. To improve the ability of particle identification will be an essential task for many important BESIII physics topics, such as, searching for $D^0$-$\overline{D^0}$ mixing and CP violation, strong phase measurements, etc. The $t_0$ extracting algorithm will make contributions to these physics topics. It can also be applied in detector calibration, for example, to precisely determine the $t_0$ offsets run-by-run with calibration data-sets.

*The authors gratefully acknowledge Dr. JIANG Lin-Li and Dr. HU Ji-Feng for their contributions to TOF reconstruction and calibration software.*

## References

1 Nelson H N. In Jaros J A, Peskin M E ed. Proc. of the 19th Intl. Symp. on Phton and Lepton Interactions at High Energy LP99. SLAC, Stanford, CA 1999

2 Bianco S, Fabbri F L, Benson D et al. Riv. Nuovo Cimento, 2003, **26N7**: 1

3 Petrov A A. eConf C030603, MEC05, 2003

4 Bigi I, Uraltsev N G. Nucl. Phys., 2001, **B592**: 92

5 Falk A F, Grossman Y, Ligeti Z et al. Phys. Rev., 2002, **D65**: 054034

6 Chua C K, Hou W S. hep-ph/0110106

7 Falk A F, Grossman Y, Ligeti Z et al. Phys. Rev., 2004, **D69**: 114021

8 Leurel M, Nir Y, Seiberg N. Nucl. Phys., 1994, **B420**: 468

9 Arkani-Hamed N, Hall L, Smith D et al. Phys. Rev., 2000, **D61**: 116003

10 YAO W M et al. Journal of Physics, 2006, **G33**: 1

11 Asner D M, Sun W M. Phys. Rev., 2006, **D73**: 034024

12 Gronan M, Grossman Y, Rosner J L. Phys. Lett., 2001, **B508**: 37

13 BESIII Design Report. Interior Document in Institute of

High Energy Physics, 2004
14 Harris F A (BES Collab.). arXiv:physics/0606059
15 LI Wei-Dong, LIU Huai-Min et al. The Offline Software for the BESIII Experiment. Proceeding of CHEP06. Mumbai, India, 2006
16 DENG Zi-Yan et al. HEP & NP, 2006, **30**(5): 371—377 (in Chinese)
(邓子艳等. 高能物理与核物理, 2006, **30**(5): 371—377)
17 Agostinelli S et al(Geant4 Collab.). Nucl. Instrum. Methods, 2003, **A506**: 250
18 RONG Gang et al. HEP & NP 2001, **25**: 154 (in Chinese)
(荣刚等. 高能物理与核物理, 2001, **25**: 154)
19 SUN Sheng-Sen, HE Kang-Lin et al. HEP & NP, 2005, **29**(2): 162—167 (in Chinese)
(孙胜森, 何康林等. 高能物理与核物理, 2005, **29**(2): 162—167)
20 JIANG Lin-Li. P.H.D Thesis, University of Sciences and Technology of China, 2006 (in Chinese)
(蒋林立. 中国科学技术大学博士论文, 2006)
21 MA Xiang et al. Nuclear Electronics & Detection Technology, to be Published(in Chinese)
(马想等. 核电子学与核探测技术, 待发表)
22 HE Kang-Lin, MAO Ze-Pu. Charged Particle Detection. Lecture on CCAST, 2006
23 HU Ji-Feng, JIANG Lin-Li et al. BES Interior Report
24 Avery P. Applied Fitting Theory I: General Least Squares Theory, CBX-91-72
25 Avery P. Applied Fitting Theory VI: Formulas for Kinematic Fitting, CBX-98-37
26 Lonnblad L et al. Comput. Phys. Commun., 1994, **84**: 307
27 HE Kang-Lin. Charm Physics Potential at BESIII. Proceeding of CLEO-c and BESIII Joint Workshop on Charm, QCD and tau Physics. Beijing, 2004, Jan.13—15
28 Feldman G J, Cousins R D. Phys. Rev., 1998, **D57**: 3873

# 利用BESIII的双层TOF寻找$D^0$-$\overline{D^0}$混合的研究*

孙永昭[1,2;1)] 何康林[1;2)] 李卫东[1;3)] 边渐明[1,2] 曹国富[1,2] 邓子艳[1] 何苗[1,2] 黄彬[1,2]
季晓斌[1] 李刚[1,3] 李海波[1] 刘春秀[1] 刘怀民[1] 马秋梅[1] 马想[1,2] 冒亚军[4] 毛泽普[1]
莫晓虎[1] 邱进发[1] 孙胜森[1] 王纪科[1,2] 王亮亮[1,2] 文硕频[1] 伍灵慧[1,2] 谢宇广[1,2]
杨明[1,2] 尤郑昀[4] 俞国威[1] 苑长征[1] 袁野[1] 臧石磊[1,3] 张长春[1] 张建勇[1,3]
张令[5] 张学尧[6] 张瑶[6] 郑志鹏[1] 朱永生[1] 邹佳恒[6]

1 (中国科学院高能物理研究所 北京 100049)
2 (中国科学院研究生院 北京 100049)
3 (中国高等科技中心 北京 100080)
4 (北京大学 北京 100871)
5 (湖南大学 长沙 410082)
6 (山东大学 济南 250100)

**摘要** 在ψ(3770)处, $D^0 \to K^-\pi^+$是研究$D^0$-$\overline{D^0}$混合的非常理想的衰变道. 实验上, 良好的K/π识别技术将对寻找$D^0$-$\overline{D^0}$混合过程起着决定性的作用. 在BESIII实验的物理预研究中, 发现利用飞行时间的信息, 能够精确测定末态中含有多条带电径迹事例的起始时间, 从而可以改善飞行时间计数器的时间分辨率. 进一步的研究表明, 应用该方法后, BESIII双层TOF的时间分辨率从∼78ps降到∼64ps. 按照$20\mathrm{fb}^{-1}$的ψ(3770)数据量进行估算, 在95%置信度下, $D^0$-$\overline{D^0}$混合率的上限值可以提高7%左右.

**关键词** $D^0$-$\overline{D^0}$混合 $D^0 \to K^-\pi^+$衰变 粒子鉴别 飞行时间计数器 事例起始时间

2006 – 08 – 29 收稿, 2006 – 10 – 30 收修改稿
∗ 中国科学院创新工程(U-602, U-34), 国家自然科学基金(10491300, 10605030)和中国科学院百人计划(U-25, U-54)资助
1) E-mail: sunyz@ihep.ac.cn
2) E-mail: hekl@ihep.ac.cn
3) E-mail: liwd@ihep.ac.cn